Case report

Multisystem Langerhans cell histiocytosis: Literature review and case report [☆],[☆☆],[★]

Cung-Van Cong, MD, PhD[a],[1], Tran-Thi Ly, PhD[b],[*], Nguyen Minh Duc, MD[c],[1],[**]

[a] *Department of Radiology, National Lung Hospital, Ha Noi, Vietnam*
[b] *Center of Training and Direction of Healthcare Activities, National Lung Hospital, Ha Noi, Vietnam*
[c] *Department of Radiology, Pham Ngoc Thach University of Medicine, Ho Chi Minh, Vietnam*

ARTICLE INFO

ABSTRACT

Langerhans cell histiocytosis (LCH) refers to a group of diseases of unknown etiology, typically discovered in childhood, characterized by the accumulation of Langerhans cells (white blood cells with large cell nuclei that may contain cytoplasmic histiocytosis X bodies) involving one or more organ systems, including bones, lungs, pituitary gland, skin, lymph nodes, and liver. This disease is also known as histiocytosis X or eosinophilic granuloma. Pulmonary LCH is common (identified in 40% of LCH patients) and may be isolated to the lung or involve other organs. Although LCH is characterized by clonal cell proliferation, adult LCH is considered likely to represent the manifestation of an aberrant immune response to an unspecified antigenic stimulus rather than a manifestation of tumor proliferation. We report a very complicated clinical case of LCH, with multiple organ damage that received a variety of different diagnoses. An LCH diagnosis was confirmed based on postoperative spinal cord pathology results and immunohistochemistry examinations. This case report highlights the clinical, laboratory, and imaging signs observed in this case that should be noted to help doctors more quickly recognize, diagnose, and treat similar cases.

Introduction

Langerhans cell histiocytosis (LCH) refers to a group of diseases of unknown etiology that manifest as the proliferation and accumulation of Langerhans cells (white blood cells with large cell nuclei that may contain cytoplasmic histiocytosis X bodies) in damaged organs. The disease can manifest in one or more organ systems, including bones, lungs, pituitary gland, mucous membranes, skin, lymph nodes, and liver. The disease is also known as histiocytosis X and eosinophilic granuloma. Pulmonary involvement is commonly observed in 40% of

patients diagnosed with LCH, which can present in either a single lung or in multiple organs. In patients with multiple organ damage, the most commonly affected sites include bones and the pituitary gland [1–3].

Most patients diagnosed with pulmonary LCH are adults (mean age 32 years). More than 90% of adults diagnosed with LCH are smokers, and the disease is thought to be related to smoking in most cases. In the early stages, pulmonary LCH is characterized by the presence of granulomas containing large numbers of Langerhans cells and eosinophils, leading to the destruction of lung tissue. LCH lesions are commonly distributed in the bronchioles. During the later stages of the disease, the granulomatous cells are replaced by pulmonary cysts and fibrosis [1,2].

Common symptoms include coughing and difficulty breathing, and up to 20% of patients present with pneumothorax. Compared with patients with multisystem disease, patients with pulmonary involvement generally have a good prognosis. The disease regresses spontaneously in 25% of cases and remains clinically and radiologically stable in 50% of cases. In the remaining 25% of cases, the disease progresses, causing extensive lung destruction and cyst formation, and patients often die due to respiratory failure or pulmonary hypertension [1].

In patients with multisystem LCH, in addition to the lungs, the most commonly affected sites include the bones and pituitary gland, whereas the involvement of other organ systems is less common. Damage to the central nervous system is particularly rare [1,2].

In this report, we describe a rare case of multisystem LCH, with the aims of contributing to the body of literature on this disease and helping doctors improve their diagnostic approaches to similar cases.

Case report

A 47-year-old woman, without history of smoking, was examined and treated at the National Lung Hospital for 1 month, presenting with headache, weakness in the lower extremities, and urinary retention. During the treatment, the patient underwent spinal surgery. It is noted that this patient was negative real-time reverse-transcriptase-polymerase chain reaction of coronavirus disease 2019 and had one-dose messenger RNA coronavirus disease 2019 vaccine.

Two months before admission, the patient was diagnosed with miliary tuberculosis (TB)-associated meningitis and type 2 diabetes at a provincial specialized hospital, where the patient was treated for tuberculosis according to the standard treatment approach. The medical establishment diagnoses tuberculosis based on chest X-ray and computed tomography (CT) scan images without bacteriological evidence. One week before admission, the patient presented with headache, weakness in the lower limbs, and low fever, but without signs of numbness, cough, or difficulty breathing. After 5 days of treatment, the patient developed urinary retention. A urinary catheter was placed, and the patient was transferred to the National Lung Hospital.

Fig. 1 – Conventional chest radiograph. Small nodules were identified predominantly in the high areas of both lungs (arow).

Upon arrival at the NHL, physical examination revealed average fitness, with no abnormalities observed upon examination of the respiratory, cardiovascular, or digestive systems. Testing for meningococcal syndrome was negative. Lower extremity muscle strength was two-fifths that of the reference value, but the patient had normal sensation in her lower extremities. Tuberculosis testing of the sputum (fluorescent acid-fast bacilli, culture, Xpert MTB) was negative. Blood counts, blood biochemistry, and urine biochemistry results were all within normal limits. Blood eosinophils were not absent. Cerebrospinal fluid tests showed a negative Gene Xpert MTB outcome at 10 TB/mm^3; protein levels at 0.69 g/L and a positive Pandy test (+); chlorine levels at 10^9 mmol/L; and glucose levels of 3.8 mmol/L. The results of microbiological tests, molecular biology with clinical signs did not support the diagnosis of tuberculosis as diagnosed by the primary health care provider.

The patient underwent a routine chest X-ray, and detailed images and film readings can be found in Fig. 1.

The patient underwent chest CT using a 64 series machine, both before and immediately after intravenous contrast injection. The contrast agent was Xenetic 350, and 100 mL was injected at 4 mL/s. The CT protocol was as follows: 139 kV; Xtube, 114 mA; slice thickness, 3 mm; window width/window level, 1200/−800 (lung window); window width/window level, 350/50 (mediastinal window). Multiplanar reconstruction was performed using 0.75-mm thin slices. The images and detailed results are presented in Fig. 2.

Because a miliary TB lesion was observed on chest CT, cranial magnetic resonance imaging (MRI) was performed, and the images and detailed film reading results are presented in Fig. 3.

Due to the patient's progressive weakness in the lower extremities, MRI of the thoracic spine was performed, revealing an abnormal oval-shaped mass, sized 15 × 24 mm, with a clear border, a hollow core, and normal organization of the surrounding pulp. MRI results and interpretations are displayed in Fig. 4.

Fig. 2 – CT chest, lung window. (A–C) Central lobar nodes are uniform in size, uniform in density, evenly distributed, and predominately located in the high areas of the lungs. (D) The low areas and costophrenic sulci are normal.
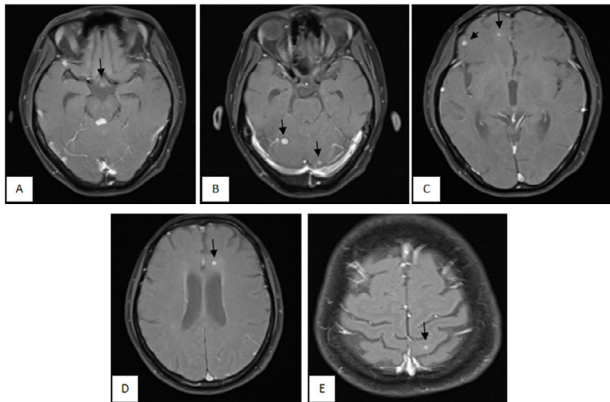

Fig. 3 – T1-weighted pulse sequence cranial magnetic resonance imaging after gadolinium injection. (A) Brainstem nodule, showing a hollow core. (B–E) Nodules (arrows) of different sizes with strong contrast enhancement were observed scattered throughout the brain, with no surrounding cerebral edema.
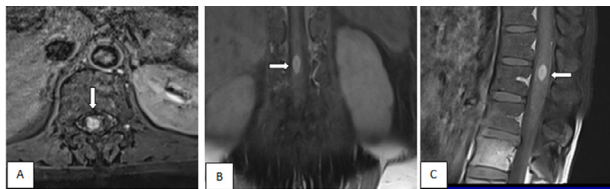

Fig. 4 – T1-weighted magnetic resonance images of the thoracic spine after gadolinium injection. An oval nodule (arrows), size 15 x 25 mm, at the D12 level was observed, with strong enhancement and a hollow core (A) Axial; (B) Coronal; (C) Sagittal.

Fig. 5 – Abnormal mass removed during spinal surgery. (A) Monolithic image, a solid, oval smooth mass sized 25 x 15 mm and ivory-white in color. (B) The specimen was cut in half, revealing a hollow center.

In response to the clinical, laboratory, and imaging data obtained to this point, many differential diagnoses were proposed, including TB in the lungs and brain; metastasis to the lungs, brain, and spinal cord; and toxoplasmosis affecting the brain and spinal cord.

Due to clinical signs of spinal cord compression, such as the weakening of the lower limbs and the potential risk of motor paralysis, a multi-specialist team was consulted, which decided to perform surgery to decompress the spine and remove the lesion from the spinal cord segment.

The operation was performed as follows. A posterior arcectomy was performed to expose the dura mater. After the dura was opened, the surgeon observed that the cerebrospinal fluid pressure increased. A longitudinal incision in the pulp body was used to remove a solid mass, oval in shape, smooth, 15 × 25 mm in size, and ivory-white in color. When cut in half, the mass was found to be hollow in the center, with no necrosis in the lumen. Suturing was performed during dural restoration, and two splints were placed along the physiological curve of the spine, strengthened by a horizontal bridge. Images of the specimens retrieved during surgery, including an illustration of the size, are shown in Fig. 5.

The specimen was examined both macroscopically and microscopically following surgery. The macroscopic examination showed an oval shape with a smooth exterior, 15 × 25 mm in size, with an ivory-white color, a hollow center, and no necrosis in the lumen. The microscopic examination revealed an inflammatory granulomatous lesion. The histopathology results were not consistent with the clinical diagnoses or imaging results, and leading pathology experts were consulted. The experts have oriented toward eosinophilic granulomata (LCH) and suggested immunohistochemical staining (Marker: CD68; S100; CD1a; CD38). Detailed images of hematoxylin and eosin staining are shown in Fig. 6.

Biopsy of the tumor area revealed histologically striated mononuclear cells, some dinuclear cells, scattered eosinophils, and macrophages consistent with fibrous stromal tissue.

Immunohistochemical test results were negative for CD1A; S100 staining revealed focally positive tumor cells; and CD68
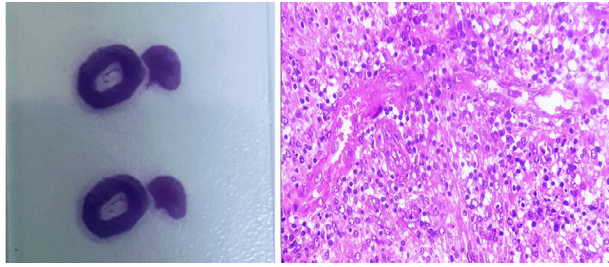
Fig. 6 – Hematoxylin and eosin staining and micrographs.

staining was positive (++). Histopathological images and immunological markers were consistent with a diagnosis of LCH.

The final diagnosis was systemic LCH lesions. Currently, the patient remains under close observation, and lower extremity mobility has improved. Corticosteroid therapy and periodic follow-up appointments are scheduled.

Discussion

LCH is a rare systemic disorder of unknown etiology characterized by the infiltration and accumulation of Langerhans cells within one or more organs. Whether LCH represents a benign neoplasm, cancer, or an immune disorder remains under debate, and the underlying pathogenic mechanism remains unclear. Diagnostic imaging and pathology play important roles in the diagnosis, monitoring, and evaluation of treatment outcomes for patients with this disease. Because the disease is characterized as a systemic disorder, multiple organ damage is often involved [1,2], and the bones, lungs, pituitary gland, mucous membranes, skin, lymph nodes, and liver are commonly affected. According to many studies, up to 40% of patients with LCH experience pulmonary manifestations (either alone or in combination with other organs). Lesions observed on chest radiograph are often nonspecific, typically displaying a nodular or reticular pattern, with bilateral injuries observed primarily in the upper and middle areas of the lungs. Lung volume may be normal or increased [2]. Chest CT can be pivotal for the diagnosis [3]. The morphological progression of lung lesions generally develops in a very characteristic sequence, beginning with the formation of small nodules, known as central lobular nodules, followed by intranodular cavitation that develops into thick-walled cysts, which eventually grow and become thin-walled. The continued growth of the cyst eventually destroys the wall, resulting in the formation of large cysts with bizarre shapes [1–7]. Nodular lesions may regress on their own or be replaced by cysts, but cystic lesions tend to persist and eventually become indistinguishable from alveolar dilatation or pneumothorax. These lesions typically appear in the upper and middle areas of the lungs and are only very rarely observed in the lower areas or in areas of the costophrenic sulci [1,7–9]. Complications may occur, especially pneumothorax, during the large cyst formation stage. Most authors have reported that lesions initially form surrounding respiratory bronchioles, followed by the distal bronchioles, and the observed cavitation in these granulo-

matous nodules is thought primarily to be due to bronchiole dilation caused by inflammation and fibrosis [1,2,10]. Brauner et al. studied high-resolution CT images obtained from 18 patients diagnosed with lung LCH over time and found that central lobar nodules appeared in 14 patients, cavernous nodules were observed in 3 patients, and thick-walled cysts were observed in 7 patients. Most lesions were diffuse (16 patients) and predominately located in the upper and middle areas of the lung, with none found in the lower regions or in the area of the ipsilateral costophrenic sulci [3]. Kim et al. conducted a study of 27 adult patients diagnosed with pulmonary LCH using longitudinal follow-up comprised of high-resolution CT and histopathology of lower lung biopsies guided by CT. The results showed that the mean patient age was 41 ± 12.3 years; small nodules were observed in 24.89% of patients; cavernous, thick-walled nodules were observed in 22.82% of patients; and cavernous, thin-walled nodules were observed in 22.82% of patients. Thin-walled cysts show a tendency to fuse with surrounding cysts, forming cysts with bizarre shapes. In particular, the biopsy results also found Langerhans cells in the walls of large cysts, associated with inflammation and active eosinophils. Following 27 patients with CT imagine, the author found that up to 14 (52%) patients showed good improvement despite active inflammatory cells detected in the cyst walls [4]. Thus, this study clearly described the regressive nature of this disease. Studies by Brauner et al. and Kim et al. also support this disease characterization [3–5]. Obert et al. performed a longitudinal study using positron emission tomography(PET)/CT with ^{18}[F]fluorodeoxyglucose to screen for systemic lesions, combined with high-resolution CT to measure respiratory function, in 14 patients with multisystem LCH over time. The results showed that at baseline, PET correctly identified all focal LCH lesions (except cecal infiltrates). The study's conclusions recommended that PET should be considered the standard tool for staging in patients with multisystem LCH. Serial PET scans are useful for assessing treatment response, especially in cases of bone LCH lesions [8].

The study by Soler et al. showed a strong association between LCH and smoking status. Diagnosis was based on the gold standard of histopathology, and smoking cessation was found to significantly reduce the risk of disease progression, with the disease regressing on its own or remaining mild but stable without requiring treatment in some cases [6].

In our case, the lung lesion was observed in the central lobular nodule stage (Figs. 1 and 2), which can be mischaracterized as nodules in the interstitial organization. The nodules were granulomatous in nature, reflecting the excessive accumulation of Langerhans cells in the respiratory bronchioles. The formation of early-stage granulomas in the lung is typically easy to observe; however, nodule formation in other organs, especially solid organs, can be difficult to detect on imaging, despite the similar nature of the lesions [4–7]. The postoperative pathology results from the spinal cord lesion revealed a granulomatous lesion. Because concordance existed between the pathological results and the lesions observed on radiographs, we opted not to perform a lung biopsy for diagnosis (which is in line with the literature); in addition, the patient continued to experience weakness in the lower extremities after surgery. The nodules in the brain and the nuclei in the spinal cord were very similar in terms of contrast enhance-

ment, and both were observed to have hollow cores, which is consistent with the progression of histiocytic nodules [3,4,6].

Multisystem LCH lesions are also common in children [9,10]. Krooks et al. showed that up to 9 of 10 pediatric LCH patients included in their study had lesions in multiple organs. Clinical signs can range from isolated, mild, and self-resolving symptoms to severe manifestations, depending on the extent of damage and dysfunction in the affected organs, especially during the initial response to treatment. Systemic symptomatic treatment combined with corticosteroids for a period of time often improves the prognosis of patients with LCH [11–16].

Spinal LCH can present with epidural or intraspinal lesions [17,18]. Lim et al. reported the case of a 28-year-old man with LCH presenting in the spinal cord. The patient reported to the clinic due to progressive weakness in lower extremity movement, gait abnormalities, back pain, and difficulty controlling the sphincter (similar to the signs observed in our patient). T2-weighted MRI showed wide, dilated canals and increased medullary signal from T2–T4. Biopsy of the lesion was performed, and histological examination of the biopsy specimens verified vascular proliferation and the significant infiltration of CD1a-positive cells, suggesting a diagnosis of LCH. The patient was successfully treated with steroid therapy [17]. Montemurro et al. also reported a case of epidural LCH with signs of canal compression [18–20]. In our case, the lesion was an abnormal nucleus located in the thoracic spinal cord, and the patient underwent spinal surgery to remove the lesion, revealing pathological results consistent with LCH. Although a few cases of diffuse LCH lesions in the spinal cord have been reported previously, mass lesions localized in the spinal cord have not been reported. To our knowledge, this is a very rare case, and similar cases have not been described in the literature. Contrast-enhanced granulomatous lesions found in the brain parenchyma are very similar to spinal cord tumors. On MRI, the granulomas were observed to be hollow in the core region, and this characteristic of LCH granuloma cavitation has not been previously reported in the literature.

Conclusion

In our rare case of systemic LCH, no obvious clinical signs of respiratory failure were observed, and no increase in eosinophils was detected. This disease manifested primarily in the lungs and central nervous system. The patient was admitted to the hospital due to headache, weakness of the lower extremities, and sphincter disorder (urinary retention on admission). Although brain lesions were detected, the cerebrospinal fluid results excluded tuberculous and meningoencephalitis. The LCH diagnosis was confirmed by immunohistochemistry of the surgical specimen retrieved from the spinal cord. In this case, the argument for a diagnosis of systemic injury may not be very rigorous (the patient did not receive a lung biopsy due to continued weakness following surgery), but concordance was observed in the imaging and clinical results. We aim to supplement the literature by describing contributions of diagnostic imaging techniques (routine radiography, CT, and MRI) during the diagnosis of this rare case.

Availability of data and materials

Data sharing is not applicable to this article as no datasets were generated or analyzed during the current study.

Authors' contributions

Cung-Van C and Nguyen MD contributed equally to this article as co-first authors. All authors read and approved final version of this manuscript.

Patient consent

Written informed consent was obtained from the patient for the publication of patient information in this article.

REFERENCES

[1] Richard Webb W, Higgins CB. Thoracic imaging: pulmonary and cardiovascular radiology. Wolter Kluwer 2017;3 E:645–57.

[2] Richard Webb W, Muller NL, Naidich DP. High – resolution CT of the lung. Wolter Kluwer 2015;5 E:492–516.

[3] Brauner MW, Grenier P, Mouelhi MM, Mompoint D. Lenoir pulmonary histiocytosis X: evaluation with high-resolution CT. Radiology 1989;172(1):255–8 PMID: 2787036. doi:10.1148/radiology.172.1.2787036.

[4] Kim HJ, Lee KS, Johkoh T, Tomiyama N, Lee HY, Han J, et al. Pulmonary Langerhans cell histiocytosis in adults: high-resolution CT-pathology comparisons and evolutional changes at CT. Eur Radiol 2011;21(7):1406–15 Epub 2011 Feb 11. PMID: 21311888. doi:10.1007/s00330-011-2075-9.

[5] Moore AD, Godwin JD, Müller NL, Naidich DP, Hammar SP, Buschman DL, et al. Pulmonary histiocytosis X: comparison of radiographic and CT findings. Radiology 1989;172(1):249–54 PMID: 2787035. doi:10.1148/radiology.172.1.2787035.

[6] Soler P, Valeyre D. Adult pulmonary Langerhans' cell histiocytosis. Rev Med Interne 2003;24(4):230–6 PMID: 12706779. doi:10.1016/s0248-8663(03)00055-9.

[7] Soler P, Bergeron A, Kambouchner M, Groussard O, Brauner M, Grenier P, et al. Is high-resolution computed tomography a reliable tool to predict the histopathological activity of pulmonary Langerhans cell histiocytosis? Am J Respir Crit Care Med 2000;162(1):264–70 PMID: 10903252. doi:10.1164/ajrccm.162.1.9906010.

[8] Obert J, Vercellino L, Van Der Gucht A, de Margerie-Mellon C, Bugnet E, Chevret S, et al. (18)F-fluorodeoxyglucose positron emission tomography-computed tomography in the management of adult multisystem Langerhans cell histiocytosis. Eur J Nucl Med Mol Imaging 2017;44(4):598–610 Epub 2016 Sep 20.PMID: 27645693. doi:10.1007/s00259-016-3521-3.

[9] Kobayashi M, Tojo A. Langerhans cell histiocytosis in adults: advances in pathophysiology and treatment. Cancer Sci 2018;109(12):3707–13 Epub 2018 Oct 30. PMID: 30281871. doi:10.1111/cas.13817.

[10] Krooks J, Minkov M, Weatherall AG. Langerhans cell histiocytosis in children: history, classification, pathobiology, clinical manifestations, and prognosis. J Am Acad Dermatol

2018;78(6):1035–44 PMID: 29754885. doi:10.1016/j.jaad.2017.05.059.

[11] Radzikowska E. Pulmonary Langerhans' cell histiocytosis in adults. Adv Respir Med 2017;85(5):277–89 Epub 2017 Oct 30.PMID: 29083024. doi:10.5603/ARM.a2017.0046.

[12] Monsereenusorn C, Rodriguez-Galindo C. Clinical characteristics and treatment of langerhans cell histiocytosis. Hematol Oncol Clin North Am 2015;29(5):853–73 Epub 2015 Aug 18.PMID: 26461147. doi:10.1016/j.hoc.2015.06.005.

[13] Néel A, Artifoni M, Donadieu J, Lorillon G, Hamidou M, Tazi A. Langerhans cell histiocytosis in adults. Rev Med Interne 2015;36(10):658–67 Epub 2015 Jul 3.PMID: 26150351. doi:10.1016/j.revmed.2015.04.015.

[14] Lian C, Lu Y, Shen S. Langerhans cell histiocytosis in adults: a case report and review of the literature. Oncotarget 2016;7(14):18678–83 PMID: 26942568. doi:10.18632/oncotarget. 7892.

[15] Menthon M, Meignin V, Mahr A, Tazi A. Adult Langerhans cell histiocytosis. Presse Med 2017;46(1):55–69 Epub 2016 Nov 2.PMID: 27816338. doi:10.1016/j.lpm.2016.09.015.

[16] Donadieu J, Héritier S. Child Langerhans cell histiocytosis. Presse Med 2017;46(1):85–95 Epub 2017 Jan 10. PMID: 28087208. doi:10.1016/j.lpm.2016.09.013.

[17] Lim CS, Cho JH. Spinal epidural involvement in adult Langerhans cell histiocytosis (LCH): a case report. Medicine (Baltimore) 2020;99(3):e18794 PMID: 32011480. doi:10.1097/MD.0000000000018794.

[18] Chan Z, Simpson L, Gallo P. Thoracic spine Langerhans cell histiocytosis in a child with achondroplasia. BMJ Case Rep 2019;12(7):e228801 PMID: 31345829. doi:10.1136/bcr-2018-228801.

[19] Montemurro N, Perrini P, Vannozzi R. Epidural spinal cord compression in Langerhans cell histiocytosis: a case report. Br J Neurosurg 2013;27(6):838–9 Epub 2013 May 22. PMID: 2369776. doi:10.3109/02688697.2013.798860.

[20] McClain KL, Picarsic J, Chakraborty R, Zinn D, Lin H, Abhyankar H, et al CNS Langerhans cell histiocytosis: common hematopoietic origin for LCH-associated neurodegeneration and mass lesions. Cancer. 2018; 124(12):2607-2620. Epub 2018 Apr 6. PMID: 29624648. doi:10.1002/cncr.31348.